Some properties of boundary layer flow during the transition from laminar to turbulent motion

By S. DHAWAN and R. NARASIMHA
Department of Aeronautics, Indian Institute of Science, Bangalore

(*Received* 28 *August* 1957)

SUMMARY

Transition in the boundary layer on a flat plate is examined from the point of view of intermittent production of turbulent spots. On the hypothesis of localized laminar breakdown, for which there is some experimental evidence, Emmons' probability calculations can be extended to explain the observed statistical similarity of transition regions. Application of these ideas allows detailed calculations of the boundary layer parameters including mean velocity profiles and skin friction during transition. The mean velocity profiles belong to a universal one-parameter family with the intermittency factor as the parameter. From an examination of experimental data the probable existence of a relation between the transition Reynolds number and the rate of production of the turbulent spots is deduced. A simple new technique for the measurement of the intermittency factor by a Pitot tube is reported.

1. INTRODUCTION

The stability of laminar shear flows and the transition to turbulent motion has received and continues to attract much attention because of its fundamental importance to the study of fluid motions. A great deal of theoretical and experimental work has been done on the instability of laminar boundary layers and in determining criteria for transition. It is known that in general transition can be influenced by the following factors: surface roughness; free stream turbulence; surface curvature; pressure gradient; surface temperature; Reynolds number; Mach number; acoustic radiation; injection or suction of fluid at the wall. Because of the complex manner in which the various factors affect transition, no satisfactory theory for the transition process has been possible so far, and the origin of turbulence is still largely an unsolved problem in fluid mechanics.

Recently, recognition of the intermittent character of laminar breakdown in a boundary layer has directed attention towards the fundamental processes involved. The observations and theoretical work of Emmons (1951) and the experiments of Mitchener (1954), Schubauer & Klebanoff (1955), Tani & Hama (1953), Hama *et al.* (1957) and others have shown that

the transition phenomenon in a boundary layer is characterized by the intermittent appearance of turbulent spots which move downstream with the fluid. The mechanics of spot creation and growth is as yet not completely clear. Experimental observations with flow visualization techniques suggest that the amplification of Tollmein–Schlichting waves becomes associated at some stage with the concentration of vorticity along discrete lines, which subsequently distort into vortex loops in the boundary layer. The vortex loops themselves go through a process of distortion and extension finally resulting in the creation of 'spots' of turbulence. Once created these spots are swept along with the mean flow, growing laterally as well as axially with laminar flow in their trail. The spots originate in a more or less random fashion and increasingly overlap as they enlarge during their transit downstream, finally covering the entire plate and resulting in fully turbulent motion. Passage of the spots over points on the surface results in alternations of laminar and turbulent flow.

These alternations can be quantitatively described by an intermittency factor γ which represents the fraction of time any point spends in turbulent flow. Flow at zero pressure gradient over a flat plate is the only case so far studied in any detail. For this case, when transition occurs naturally or due to a disturbing agency which causes the spots to appear at some distance downstream, the spots grow laterally in a nearly linear manner sweeping 'turbulence wedges' on the plate. The angle of these wedges is approximately the same as that for transverse contamination found by Charters (1943). During the initial period the spot growth is non-linear, and envelopes of spot growth exhibit a characteristic curved shape.

The existence of turbulent spots in boundary layer flow has been confirmed experimentally by Mitchener (1954), Schubauer & Klebanoff (1955) and in this laboratory, and it appears to be quite certain that their occurrence plays a fundamental role in the mechanics of boundary layer transition and probably also in the breakdown of laminar motion in general. In this paper the transition region of a boundary layer on a flat plate is examined from a viewpoint which keeps the intermittency of flow as the central feature of the process. It is then sought to utilize the available experimental and analytical information to explain details of the flow in the boundary layer during transition. The main sources of experimental information on the mechanics of transition utilized for analysis here are the experiments by Schubauer & Klebanoff (1955) at the Bureau of Standards, Washington, D.C., and those conducted at the Indian Institute of Science, Bangalore. Both sets were carried out in low-turbulence wind tunnels under carefully controlled environmental conditions.

In the literature it is indeed rare to find transition measurements which provide sufficiently complete information. The most serious omission in the older studies is usually the intermittency factor whose significance was probably not recognized earlier. It is hoped that such measurements will become more common in the future, and will provide more extensive data on transition flows.

2. Distribution of intermittency during transition

Experimentally, distributions of the intermittency factor during a transition zone can be measured by placing a hot-wire close to the surface and recording the amplified output on an oscillograph. Typical records obtained in this manner are shown in figure 1 (plate 1). The passage of each spot over the hot-wire is characterized on the oscillographs by random high-frequency fluctuations in contrast to the relatively regular, smooth laminar regions. The factor γ is easily calculated from such records by counting the intervals of time for which the traces show turbulent flow.

For a quantitative description of the transition process, Emmons (1951) has formulated a theory based on probability considerations. This theory assumes the existence of a turbulence spot production function $g(x, y, t)$, and Emmons shows how this can be related to the probability of the flow being turbulent at some point, i.e. to the intermittency factor γ. It has been shown by Narasimha (1957) how the original assumptions about the production of turbulence sources have to be modified in the light of new observations. The main feature of the modification stems from observations which suggest that laminar breakdowns in a two-dimensional flat plate boundary layer are very nearly point-like, and that the spots originate in only a restricted region. On physical grounds which have some support from stability theory, one may argue that the amplified laminar oscillations can be expected to lead to production of the turbulent spots at a fairly definite distance from the leading edge of the plate. Since the actual occurrence of spots is random, one can reason that there must be a region on the plate downstream of the point of instability where the origin of the spots is most probable. At points further downstream, the tendency for breakdown rapidly decreases on account of the state of flow behind a spot as well as the fact that most of the breakdowns have already occurred. Thus the source-rate density function describing spot production should have a maximum at some location. It turns out that the experimentally observed beginning of transition marks this location.

If one assumes a Gaussian error curve with its maximum at x_t to describe the turbulence source-rate function, then Emmons' theory can be used to calculate the resulting γ distributions. Here x_t is the location where transition begins. It is interesting to note that the Gaussian curve which gives the best agreement with experimental data has a standard deviation approaching zero. This implies the form of the source-rate function to be very nearly the Dirac delta function. Figures 2 (*a*) and 2 (*b*) show representative cases of transition illustrating calculations based on the above arguments. An interesting and important feature of this hypothesis of localized laminar breakdown is the explanation it suggests for the observed statistical similarity in the transition distributions. Application of this hypothesis together with Emmons' theory gives

$$\gamma = 1 - e^{-A\xi^3}. \tag{1}$$

Here $\xi = (x - x_t)/\lambda$, a normalized stream-wise coordinate in the transition

zone, λ being a measure of the extent of the transition region characterized by

$$\lambda = \{x\}_{\gamma=0\cdot75} - \{x\}_{\gamma=0\cdot25},$$

and A is a constant equal to 0·412.

Equation (1) shows that whatever the cause of transition, all transition regions define a single universal intermittency distribution. Figure 3 shows the available data on intermittency during transition, and demonstrates the agreement between equation (1) and experiment. Further experimental

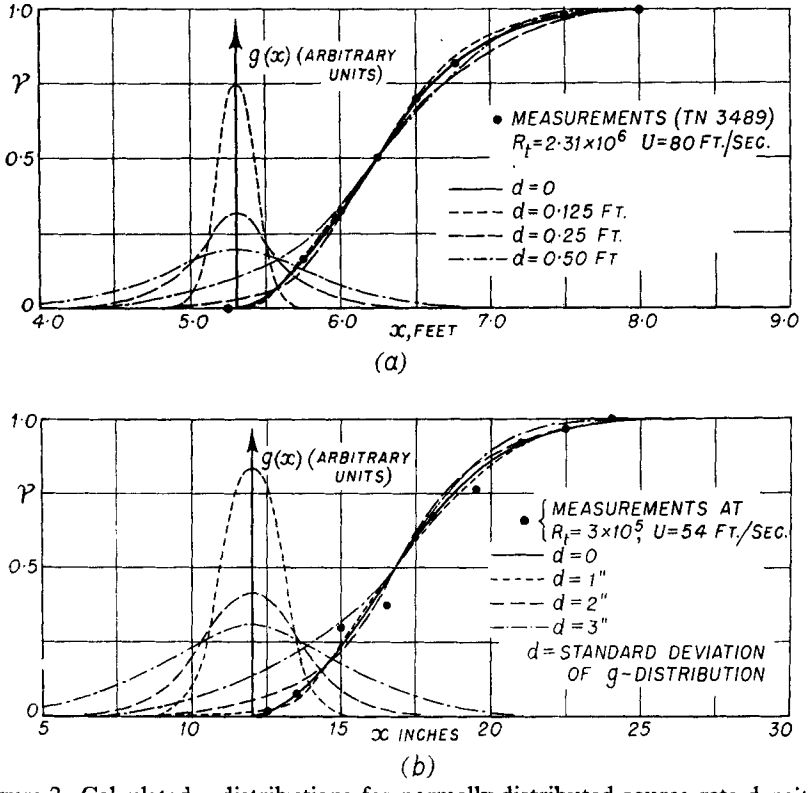

Figure 2. Calculated γ-distributions for normally distributed source-rate density.

evidence supporting the view that the origin of most of the turbulent spots is very close to the beginning of transition is given by observations of boundary layer thickness during transition. Figure 4 shows two representative cases. They reveal that the virtual origin of the resulting turbulent boundary layer is very nearly at x_t. The effect of pressure gradients on the $\gamma(\xi)$ distributions has not yet been investigated in detail, but preliminary measurements indicate that the distribution is modified mainly in the neighbourhood of $\gamma = 0$. Pressure gradients would thus appear to chiefly influence the manner of spot growth in the initial period.

Another point of interest is the distribution of γ across the boundary layer, viz. normal to the plate surface. Note that $\gamma(y)$ is a function of the shape of the turbulent spots. The very detailed experiments of Schubauer & Klebanoff (1955) and measurements in this laboratory show that the spots

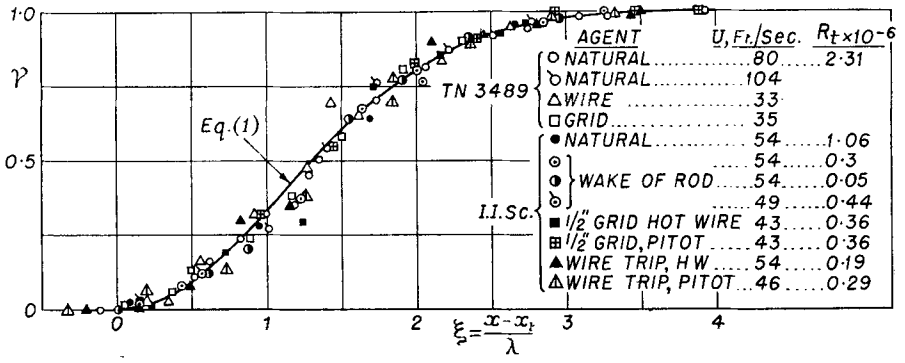

Figure 3. Universal distribution of γ *vs* ξ with transition due to different agents.

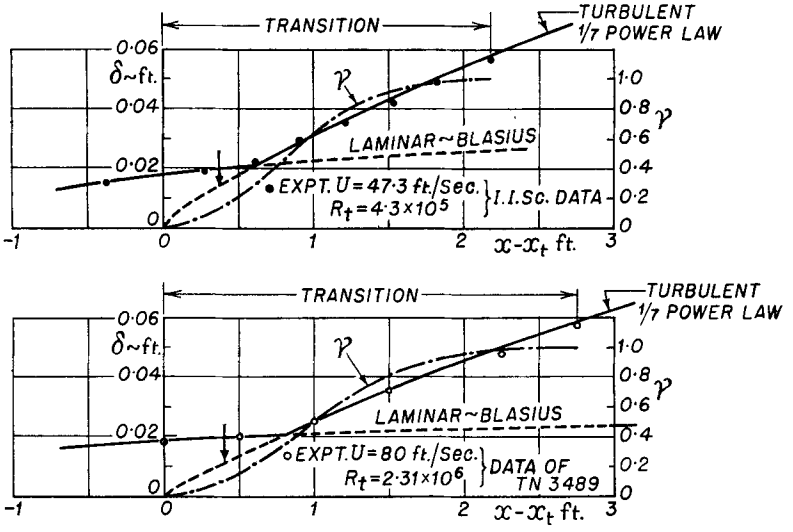

Figure 4. Boundary layer thickness in transition region (arrows mark limit of logarithmic turbulent boundary layer).

have a nearly constant cross-sectional area close to the surface, but they taper towards the outer edge. The measured $\gamma(y)$ distributions during transition are similar to those observed by Corrsin & Kistler (1954) in fully developed turbulent boundary layers, i.e. γ varies from a constant maximum value close to the wall to zero towards the edge. While this $\gamma(y)$ variation is probably of importance to the detailed structure of the turbulent motion associated with the spots for all practical purposes, the γ value near the wall is the characteristic property of importance for the

transition region. For instance, it is seen in § 3 that the $\gamma(y)$ variation has only a secondary influence in determining the mean velocity profiles in transition.

To sum up, it would appear that the almost point-wise breakdown of laminar flow in a boundary layer while occurring randomly in time takes place very nearly on a discontinuous line across the flow, whatever the cause of breakdown may be.

3. Details of transition flow

(*a*) *Location and extent of the transition zone*

It has been observed in § 2 that the distribution of intermittency is universal on the $\gamma(\xi)$ plot, This implies that the transition zone has always the same extent in terms of the ξ-coordinate. This information tells us nothing about the physical location of the beginning of the transition region. So far it is not possible to predict theoretically, even in the simplest case, the Reynolds number of transition R_t. Since the mechanics of creation of the turbulent spots has yet to be formulated, attempts such as those by Liepmann (1945) and Lees (1952) to estimate R_t from the development of amplified laminar oscillations lead to difficulties and have not yet been too successful. Experimental investigations have established useful correlations for the effect of particular types of disturbance agencies on R_t (see Dryden (1953), Gazley (1953) and Lin (1955) for recent reviews of the available information). There are, however, unexplained discrepancies, and in any case these correlations are not general enough to predict R_t when there is a combination of transition agencies.

A recent study of the experimental data on boundary layer transition available in the literature shows the possible existence of an interesting relation between the transition Reynolds number R_t and R_λ, the Reynolds number based on the physical extent of the transition zone. Figure 5 shows a plot of R_λ *vs* R_t for the available experimental data. Since in many cases there were unspecified differences in experimental conditions, the data show considerable scatter; but in spite of this one can discern the dependence of R_λ on R_t. The extent of the transition zone appears to decrease progressively with decreasing R_t, to some limiting value. Actually one would expect a family of R_λ *vs* R_t curves with each curve depending on the specific agency or agencies causing transition and each having perhaps different limiting values. Figure 5, however, shows that this dependency on the type of disturbance is not too marked, and that for rough estimates a single mean curve may be used. The data are represented on the average by the equation

$$R_\lambda = \alpha R_t^\beta \tag{2}$$

with $\alpha = 5{\cdot}0$ and $\beta = 0{\cdot}8$.

It should be noted that R_λ is related to the turbulence source-rate production function of Emmons, and the possible existence of an R_λ *vs* R_t relation is probably of some significance to the transition problem. Using

equation (2), it is possible to calculate $\tilde{n}$, the average number of turbulence sources produced per second, as a function of the transition Reynolds number. The results of this calculation are shown as an $\tilde{n}$-scale in figure 5.

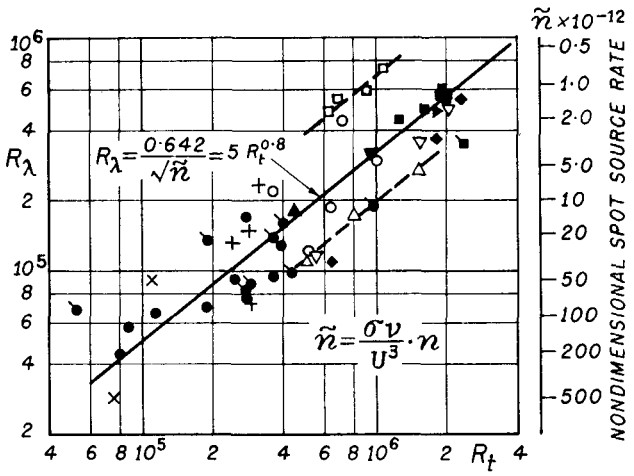

Figure 5. Correlation between R_t and R_λ. (Flagged points are hot-wire measurements.)

Subsonic measurements

- ● Indian Inst. Sci.
- ■ Schubauer & Skramstad (1947), Schubauer & Klebanoff (1955).
- ▲ Dhawan (1953).
- ◗ Hunsaker (1939).
- \+ × Burgers (1925).

} flat plate

- ■ Wright & Bailey (1939), flat plate with pressure gradient.
- ▼ Silverstein & Becker (1939), aerofoil.

Supersonic measurements

- ○ Coles (1954), flat plate, $M = 1{\cdot}97$–$4{\cdot}54$.
- □ Higgins & Pappas (1951), flat plate, $M = 2{\cdot}4$.
- ▽ Chapman & Kester (1953), cone-cylinder, $M = 2{\cdot}9$.
- △ Winter *et al.* (1954), cone, $M = 2{\cdot}45, 3{\cdot}25$.

(*b*) *Mean velocity profiles in the boundary layer during transition*

Following the discussions of § 1 and § 2, we note that each point on the flat plate during transition is covered with a laminar boundary layer except during those intervals of time when turbulent spots pass over it. Two questions of immediate interest are: (i) what velocity profile is associated with a turbulent spot during its motion; and (ii) whether the mean velocity profiles during the intermittent transition process exhibit any similarity.

The clue to these and other related questions is contained in the observations which show that the turbulent spots are randomly created at a fairly definite x-wise location, and are on the average all similar in shape, their propagation cones being very nearly true cones with straight generators.

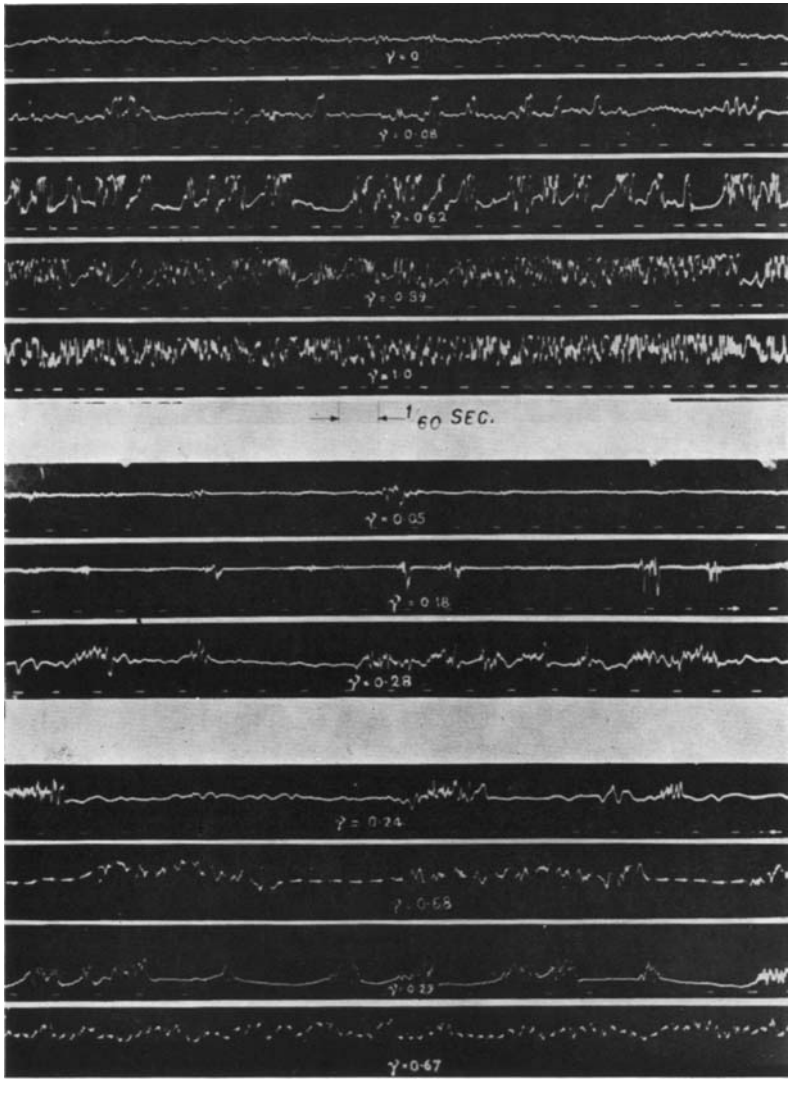

$\gamma(x)$ at $y = 0{\cdot}012$ in.
Transition due to 0·013 in. dia. wire trip

$\gamma(y)$ at $x = 4{\cdot}25$ ft. Natural transition

Natural transition

Transition due to 2 mesh screen

Transition due to isolated roughness element

Transition due to wake of $\frac{1}{8}$ in. dia. rod

Figure 1. Specimen hot-wire records.

The fully turbulent boundary layer on the plate which results after transition exhibits the characteristics of a two-dimensional turbulent layer, because it is a random mix-up of the turbulent spots originating from a narrow localized region. Within the transition zone one can similarly associate, on the average, a two-dimensional boundary layer with each spot, since the transition boundary layer is also a random mix-up of the spots but for smaller intervals of time. The overall effect, therefore, is approximately equivalent to a flow in which, at each point, the boundary layer alternates between a two-dimensional laminar and a two-dimensional turbulent layer, each at its appropriate Reynolds number, γ representing the proportion of time spent in turbulent motion. The origin of the laminar layer is at the leading edge of the plate, while γ departs from its zero value at some point further downstream. The thickness of the transition boundary layer would be equal to the laminar or the turbulent layer starting from x_t, whichever is the greater.

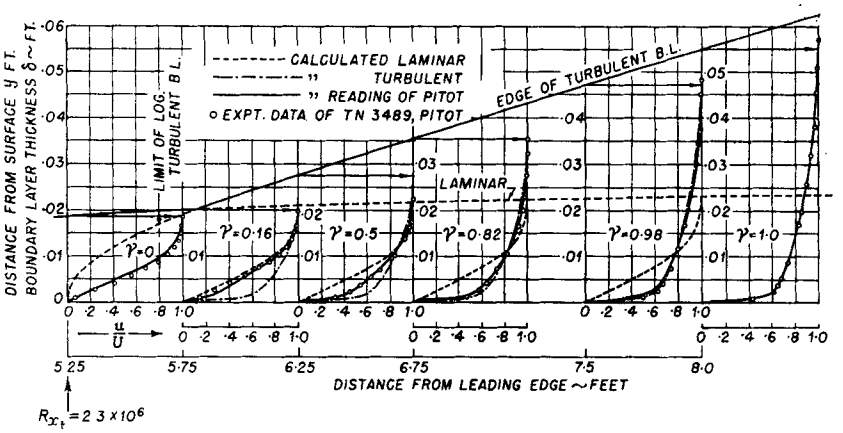

Figure 6. Boundary layer velocity profiles in transition.

Analysis of carefully obtained experimental data confirms the above observations. Figure 4 shows two representative cases of transition flow, and it is seen that the observed thickness of the transition boundary layer closely checks estimates based on the above reasoning. Figure 6 shows a case of transition analysed in detail. The calculated laminar and turbulent profiles between which the flow alternates are shown for each station on the plate where a mean profile was measured with a total-head tube. Also shown on the figure are the calculated mean Pitot profiles obtained by mixing the laminar and turbulent flows.

The agreement between the measurements and the calculations supports the basis of the arguments outlined above. The calculated turbulent boundary layer profiles are based on a combination of the well-known 'law of the wall' and the 'velocity defect law' as discussed by Clauser (1956). The constants entering into these laws were determined in each case from the measured fully developed turbulent profiles. Figures 4 and 6

show that the logarithmic turbulent profile is attained in the turbulent spots quite early in the transition process. The behaviour of turbulent boundary layers at low Reynolds numbers being not very well understood, the deviation of the calculated profiles from the experimental data at low γ values is not surprising. The calculations can give only an approximate indication of the state of flow during the early history of a spot.

The Pitot profiles $u_P(y)$ during transition were calculated from the equation

$$u_P(y) = \{(1-\gamma)u_L^2 + \gamma u_T^2\}^{1/2}, \tag{3}$$

γ being measured independently by hot-wire techniques and u_L, u_T being the theoretical laminar and turbulent profiles respectively. Equation (3), incidentally, indicates that in regions of intermittent flow care must be exercised in interpreting the readings of averaging instruments such as Pitot tubes and hot-wire anemometers. The reading of a Pitot is proportional to pressure (u^2); hence the average velocity during transition flow indicated by a Pitot tube (i.e. equation (3)) is different from the true time mean $\bar{u}$, which is given by

$$\bar{u} = (1-\gamma)u_L + \gamma u_T. \tag{4}$$

Equations (3) and (4) are compared in figure 7, which shows a representative transition velocity profile measured carefully by means of a small flat total-head tube. A complete $\gamma(y)$ distribution measured across the boundary layer at the same location is also included.

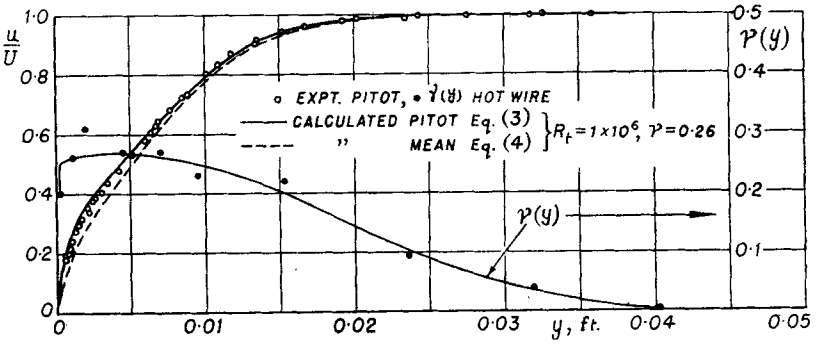

Figure 7. Transition profile.

Significant facts which emerge from the data and calculations of figures 6 and 7 are as follows:

(*a*) The calculated Pitot profiles are in remarkable agreement with the reading of the total-head tube. This agreement proves the soundness of the physical picture on which the analysis is based.

(*b*) Although γ varies across the boundary layer, for purposes of profile calculation, the value measured close to the wall gives sufficiently accurate results for the whole profile. Thus the spot shape which is associated with the $\gamma(y)$ variation appears to have only a secondary influence on the transition flow, $\gamma(x)$ being the significant property.

(*c*) Transition velocity profiles measured with a total-head tube must be corrected to give the mean profile. The errors are specially significant close to the wall, and skin friction determinations from uncorrected measured profiles are likely to have large errors.

Before taking up the question of similarity of the mean velocity profiles during transition, it is useful first to consider the boundary layer parameters δ^*, θ, H which are known to play an important part in the quantitative description of boundary layers. During transition the displacement and momentum thickness can be defined as

$$\delta_t^* = \int_0^{\delta_t} \left(1 - \frac{\bar{u}}{U}\right) dy, \tag{5}$$

and

$$\theta_t = \int_0^{\delta_t} \frac{\bar{u}}{U}\left(1 - \frac{\bar{u}}{U}\right) dy, \tag{6}$$

where δ_t is the thickness of the transition boundary layer, and $\bar{u}(y)$ is given by (4). U is the uniform velocity outside the boundary layer.

Using (4) in (5) and (6), and recognizing that $\delta_t = \delta_L$ if $\delta_L > \delta_T$, or $\delta_t = \delta_T$ if $\delta_T > \delta_L$, we obtain after some simplification

$$\delta_t^* = (1-\gamma)\delta_L^* + \gamma(\delta_T^*), \tag{5 a}$$

and

$$\theta_t = (1-\gamma)\{(1-\gamma)\theta_L - \gamma\delta_L^*\} + \gamma\{\gamma\theta_T - (1-\gamma)\delta_T^*\} + 2\gamma(1-\gamma)F(\delta_t), \tag{6 a}$$

where δ_L^*, δ_T^* are displacement thicknesses and θ_L, θ_T are momentum thicknesses of the laminar and turbulent profiles respectively, and

$$F(\delta_t) = \int_0^{\delta_t} \left[1 - \left(\frac{u}{U}\right)_L \left(\frac{u}{U}\right)_T\right] dy.$$

Figure 8 shows two cases of transition flow for which equations (5 a) and (6 a) have been compared with experimental data obtained from corrected profiles and γ measurements. One set of corrected profiles measured for $R_t = 4{\cdot}3 \times 10^5$ is shown in figure 9, while the other set for $R_t = 2{\cdot}3 \times 10^6$ is the same as that shown in figure 6. The analysis is seen to give good agreement with the measured distributions of δ_t^* and θ_t. The profile-shape parameter H is given by

$$H_t = \delta_t^*/\theta_t, \tag{7}$$

and this can be put in the form

$$H_t = \frac{(1-\gamma)H_L + \gamma H_T \dfrac{\theta_T}{\theta_L}}{(1-\gamma)^2\left[1 - \dfrac{\gamma}{1-\gamma} H_L\right] + \gamma^2\left[1 - \dfrac{1-\gamma}{\gamma} H_T\right]\dfrac{\theta_T}{\theta_L} + 2\gamma(1-\gamma)\dfrac{F}{\theta_L}}, \tag{7 a}$$

where H_L and H_T are the form parameters for the laminar and turbulent boundary layers respectively.

The variation of H_t is shown in figure 8 for the two cases studied. It is interesting to note that when plotted against the ξ-coordinate, the variation of H_t in the transition region shows a near universality. Actually, as the

figure shows, one can notice a small Reynolds number effect on H_t mainly towards the latter half of transition. This is to be expected since the turbulent boundary layer associated with the spots depends on R_t, the Reynolds number of transition, and H for the turbulent layer is known to vary with Reynolds number. Figure 8 shows that the effect on H_t is small

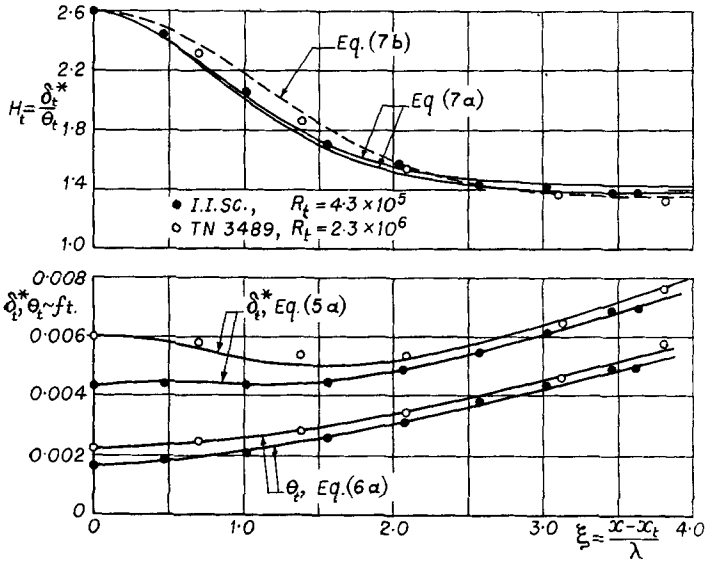

Figure 8. Boundary layer parameters during transition.

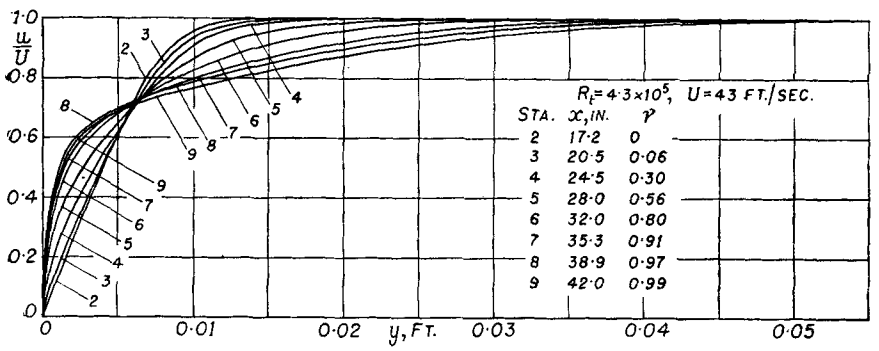

Figure 9. Corrected mean transition profiles (Indian Inst. Sci.).

for a wide range of R_t values. For approximate calculations, a simple expression can be derived for the distribution of the transition-shape parameter. This is of the form

$$H_t = H_T + (H_L - H_T)e^{-A\xi^2}. \tag{7b}$$

This expression implies a linear relation between H_t and γ, and is plotted in figure 8 for comparison.

Having seen that a knowledge of R_t and $\gamma(x)$ for any case of transition leads to a calculation of the mean velocity profiles as well as the parameters δ_t^*, θ_t and H_t, we now attempt to represent the profiles as far as possible in a unique manner. It is known from boundary layer theory that for steady flow past a flat plate with zero pressure gradient, both the laminar as well as the fully developed turbulent boundary layers exhibit similarity. This fact is usually expressed by the profiles being independent of Reynolds number effects when expressed in the form

$$\left(\frac{u}{U}\right)_L = f\left(\frac{y}{\theta_L}\right), \tag{8}$$

and

$$\left(\frac{u}{U}\right)_T = g\left(\frac{y}{\theta_T}\right). \tag{9}$$

The function $f(\ )$ is defined by the Blasius solution, while $g(\ )$ can be tabulated in terms of the nearly universal turbulent boundary layer logarithmic laws, of which the $\frac{1}{7}$th power law is an approximate representation. Since the mean transition profiles are a resultant of the

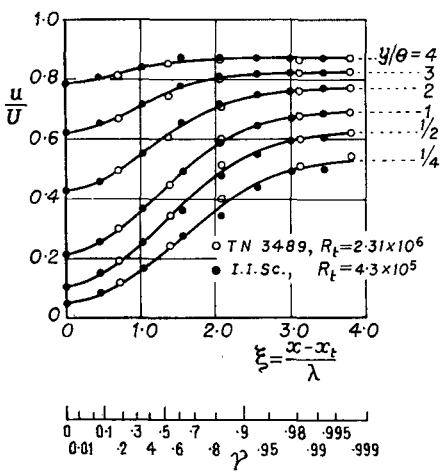

Figure 10. Similarity of transition profiles.

laminar and turbulent profiles combined in proportion to γ, it is logical to extend the similarity of equations (8) and (9) to transition flow by including the effect of γ. We thus postulate that

$$\left(\frac{\bar{u}}{U}\right)_t = h\left(\frac{y}{\theta_t}, \gamma\right). \tag{10}$$

In principle the function $h(\ )$ is defined by a solution of the differential equations governing the mean transition flow. Unfortunately, these have yet to be formulated. We resort to an examination of experimental data for information on the form of $h(\ )$.

In figure 10 two sets of mean transition profiles measured for widely differing R_t have been plotted in the form $(\bar{u}/U)_t$ *vs* ξ for fixed values of

y/θ. Since ξ is a function of γ, a γ-scale is also shown. Figure 10 shows that the transition profiles do indeed define, at least approximately, a function $h(y/\theta, \gamma)$ which for all practical purposes is independent of Reynolds number. Figure 11 is a cross-plot from figure 10, and shows the universal laminar and turbulent transition profiles as well as the one-parameter family of profiles. Persh (1955) has noted, from an examination of experimental data, that transition profiles exhibit approximate parametric similarity when plotted as u/U *vs* H for fixed y/θ. We recall from (7 b) that $H_t(\xi)$ is nearly independent of Reynolds number effects. Since the functions $\gamma(\xi)$ and $h(y/\theta_t, \gamma)$ are universal, the reasons for the correlation observed by Persh become clear. The representation of transition profile data in the form of equation (10) is to be preferred as it shows the dependence on intermittency explicitly.

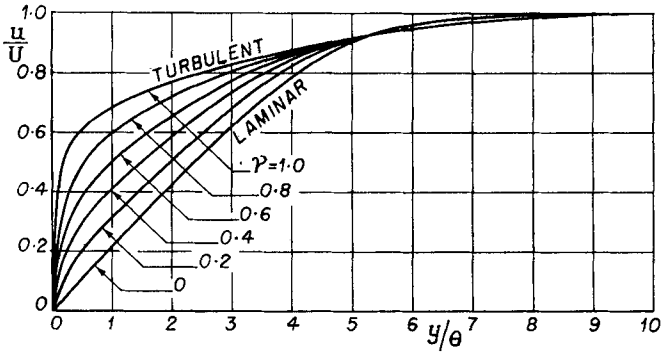

Figure 11. Similarity of transition profiles; $(\bar{u}/U)_t = h(y/\theta_t, \gamma)$.

(*c*) *Skin friction*

Local skin friction

If c_{f_L} and c_{f_T} are the local skin friction coefficients for laminar and turbulent flow respectively, then the mean local skin friction during transition is given by

$$c_{f_t} = (1-\gamma)c_{f_L} + \gamma c_{f_T}. \tag{11}$$

This equation is plotted in figure 12 for the two cases of transition analysed earlier. The transition c_f-curves, which fair smoothly into those for laminar and turbulent flow, show a more rapid increase of wall friction than is usually assumed. At the end of transition the local skin friction is seen to be considerably higher than the values given by the turbulent skin friction laws based on the turbulent boundary layer starting at the leading edge of the plate. The usual presentation of skin friction data on a plot of the total friction coefficient C_F *vs* R_x obscures the fact that the origin of the turbulent boundary layer is approximately coincident with the beginning of transition and the onset of intermittency. The usual skin friction curve for turbulent flow must be translated along R_x so that its virtual origin coincides with the foot of transition.

Independent evidence supporting this is provided by the transition local skin friction data of Coles (1954), which is shown in figure 13. Coles' experiments measured c_{f_t} directly, and were conducted at supersonic speeds so that the final turbulent boundary layer curves must include compressibility corrections. In figure 13 the Frankl–Voishel (1943) theoretical curve for c_{f_T} has been used as this is known to give reasonably accurate predictions of supersonic skin friction. The characteristic shape

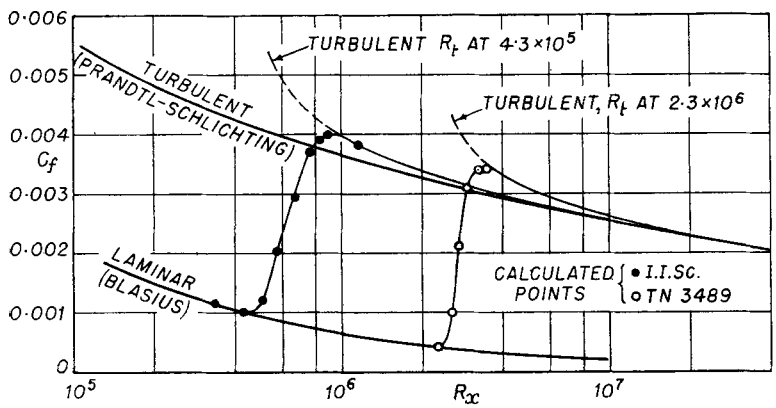

Figure 12. Local skin friction in transition region.

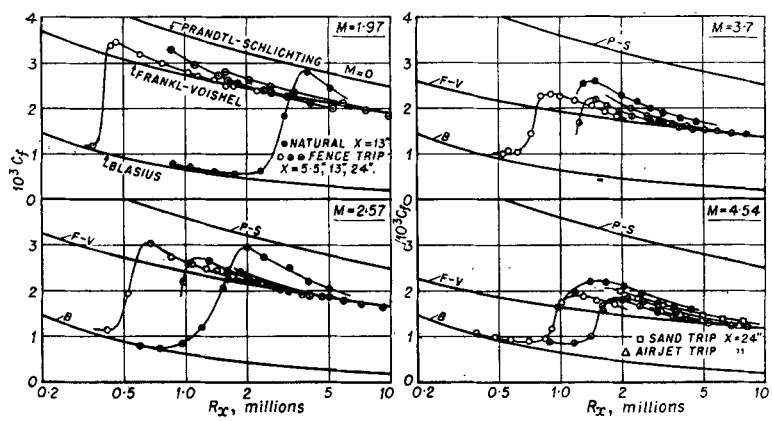

Figure 13. Local skin friction during transition in supersonic flow (from Coles 1954).

of the local c_f curves rising above the turbulent friction curves is seen again. These data also suggest that the mechanism of transition is not altered at supersonic speeds. The fact that after the breakdown of laminar flow the resulting turbulent boundary layer has an effective origin close to the beginning of transition resulting in high c_f values is probably also the reason why measurements of transition recovery factors show values higher than expected (Shoulberg, Hill & Rivas 1954).

Another interesting feature of the transition local skin friction curves is brought out by figure 14, which shows that the difference $\{c_{f_t} - c_{f_t}|_{\gamma=0}\}$ is independent of Reynolds effects during transition. Here $c_{f_t}|_{\gamma=0}$ is the value of c_{f_L} at x_t. The points shown on figure 14 were calculated from the corrected experimental profiles used elsewhere in this paper. They approximately define a single curve with ξ as the variable. While it is difficult to give an *a priori* theoretical justification for this observed correlation, a reasonable explanation is as follows.

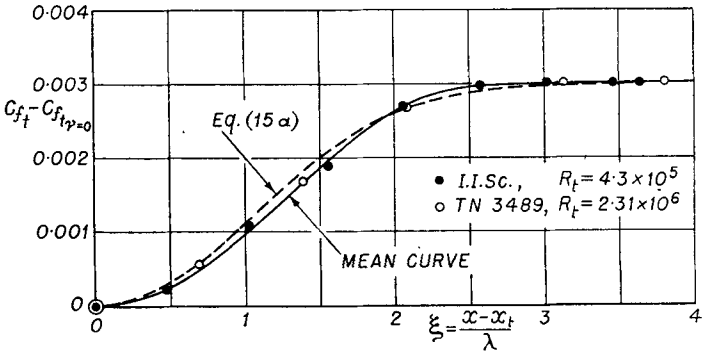

Figure 14. Similarity in variation of skin friction during transition.

We have that in (11) c_{f_L} and c_{f_T} may be represented as

$$c_{f_L} = K_1/R_x^{1/2}, \tag{12}$$

$$c_{f_T} \doteq K_2/R_x^{1/5}, \tag{13}$$

where K_1, K_2 are constants. Using the definition of ξ and equations (1), (12) and (13), we can write (11) as

$$c_{f_t} = F\{R_t, R_\lambda, \xi\}. \tag{14}$$

Now if R_t and R_λ are related as suggested by the experimental data of figure 5, equation (14) becomes

$$c_{f_t} = F\{R_t, \xi\}. \tag{14a}$$

The correlation observed in figure 14 shows this function to have the form

$$F\{R_t, \xi\} = \Phi(R_t) + \Psi(\xi) \tag{14b}$$

with $\Phi(R_t) = c_{f_t}|_{\gamma=0}$, the value of laminar skin friction at the beginning of transition.

We thus get

$$c_{f_t} - c_{f_t}|_{\gamma=0} = \Psi(\xi), \tag{15}$$

function of the ξ-coordinate alone. We note that figure 14 implies, once again, that the main Reynolds number effect on transition is through the location of the region of laminar breakdowns. Subsequent events are

controlled by the intermittency and its distribution. An approximate expression for the function Ψ is

$$\Psi(\xi) = 0{\cdot}003(1-e^{-\frac{1}{2}\xi^2}). \tag{15 a}$$

This equation is plotted in figure 14.

Total skin friction

The behaviour of the local skin friction coefficient during transition discussed above can be used for engineering purposes to calculate the total skin friction of a plate on which transition occurs at some location. Integration of (11) for a plate of length l with transition starting at $x = x_t$ and ending at $x = x_t'$ gives

$$\left.\begin{aligned} C_F &= \frac{1}{l}\int_0^l c_f\,dx \\ &= \frac{x_t}{l}\int_0^{x_t} c_{f_L}\,dx + \frac{\lambda}{l}\int_0^{\xi} c_{f_t}\,d\xi, && \text{for } l \leqslant x_t', \\ &= \frac{x_t}{l}\int_0^{x_t} c_{f_L}\,dx + \frac{\lambda}{l}\int_0^{4\cdot0} c_{f_t}\,d\xi + \frac{1}{l}\int_{x_t'}^{0} c_{f_T}\,dx, && \text{for } l > x_t'. \end{aligned}\right\} \tag{16}$$

Here the upper limit of the second integral for $l > x_t'$ has been taken to be $\xi = 4{\cdot}0$ in accordance with figure 3.

These expressions may be put in a more convenient form by utilizing the approximate relation (15 a) and the R_t *vs* R_λ relation of (2). The total skin friction coefficient C_F is then given by

$$\left.\begin{aligned} C_F &= \frac{a+bR-C\,\mathrm{erf}(dR'/R_t^\beta)}{R_l}, && \text{for } l \leqslant x_t', \\ \text{and} \\ C_F &= \frac{R'C_{F_T}-k}{R_l}, && \text{for } l > x_t', \end{aligned}\right\} \tag{16 a}$$

where

$$a = R_t\{C_{F_L}|_{\gamma=0}\}, \qquad b = 0{\cdot}003 + C_{F_L}|_{\gamma=0},$$

$$C = 0{\cdot}00376\alpha R_t^\beta = 0{\cdot}0188R_t^{0{\cdot}8}, \qquad d = 0{\cdot}707/\alpha = 0{\cdot}141,$$

$$k = C-a+4\alpha R_t^\beta\{C_{F_T}|x_t'-b\} = 5\{0{\cdot}00376+4(C_{F_T}|x_t'-b)\}R_t^{0{\cdot}8}-a,$$

$$\alpha = 5{\cdot}0, \qquad \beta = 0{\cdot}8, \qquad R' = R_x - R_t,$$

$$\mathrm{erf}\,z = \frac{2}{\sqrt{\pi}}\int_0^z e^{-s^2}\,ds.$$

Equation (16 a) is plotted for a range of R_t values in figure 15. For one case a comparison is shown with Emmons' calculations, the usual Prandtl–Schlichting estimation, and Geber's experimental data (see Schlichting 1955). The present analysis shows a sharper rise of C_F due to transition than is indicated by Emmons and shows a rounding-off of the transition curve at the beginning of transition unlike the Prandtl–Schlichting semi-empirical curve.

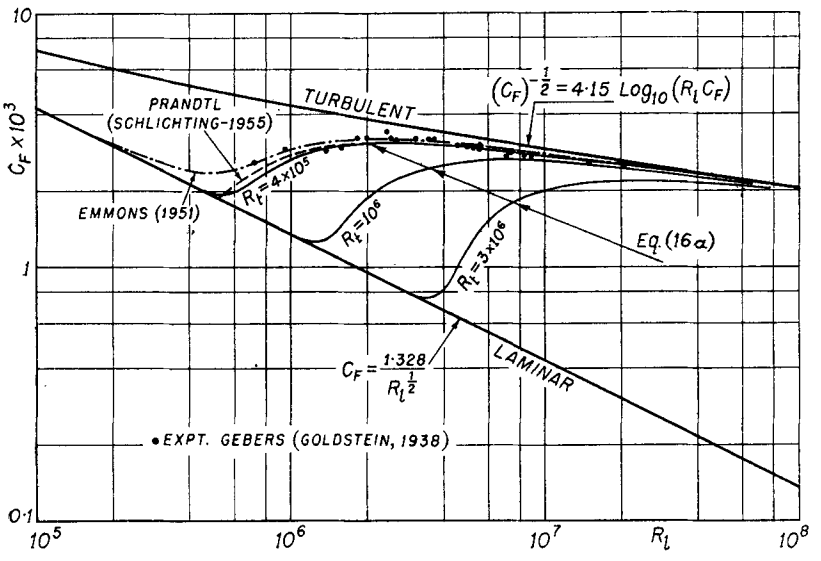

Figure 15. Mean friction coefficient of a flat plate with transition at R_t.

4. Estimation of γ by a Pitot tube

It has been shown in § 3 that fairly good agreement is obtained between the velocity profiles measured by a Pitot tube and those calculated from the formula (obtained immediately from (3))

$$\left(\frac{u}{U}\right)_P = \left\{(1-\gamma)\left(\frac{u}{U}\right)_L^2 + \gamma\left(\frac{u}{U}\right)_T^2\right\}^{1/2}$$

using measured values for γ and the theoretically known values for $(u/U)_L$ and $(u/U)_T$. This immediately suggests the possibility of experimentally obtaining γ without having to use the hot wire and associated equipment. From the measured velocity profile, or indeed from a single measurement of $(u/U)_P$ in the transition region at a certain height from the surface, γ can be obtained as

$$\gamma = \frac{\left(\frac{u}{U}\right)_P^2 - \left(\frac{u}{U}\right)_L^2}{\left(\frac{u}{U}\right)_T^2 - \left(\frac{u}{U}\right)_L^2}, \tag{17}$$

where $(u/U)_P$ is the reading of the Pitot tube.

A suitable procedure for determining the γ-distribution by this method is to traverse a Pitot tube along the transition region at a fixed height above the surface. To get the best results, the height should be such that the difference in the velocity, at that height, between the laminar and turbulent profiles is as large as possible throughout the transition region. From an examination of figures 9 and 10, it seems that this height should be of the order of θ. A surface tube is not likely to give satisfactory results, as its readings cannot always be quantitatively interpreted.

Figure 16 compares intermittency measurements obtained for the same flow by the hot wire and Pitot methods. For the latter, the velocities $(u/U)_p$ were read off, for a height from the surface of 0·024 in., from measured Pitot velocity profiles. Figure 17 shows the results obtained from a Pitot traverse at a height of 0·035 in., together with the calculated laminar and turbulent curves. The origin for the turbulent boundary layer was chosen as the point where the measured curve departs from the

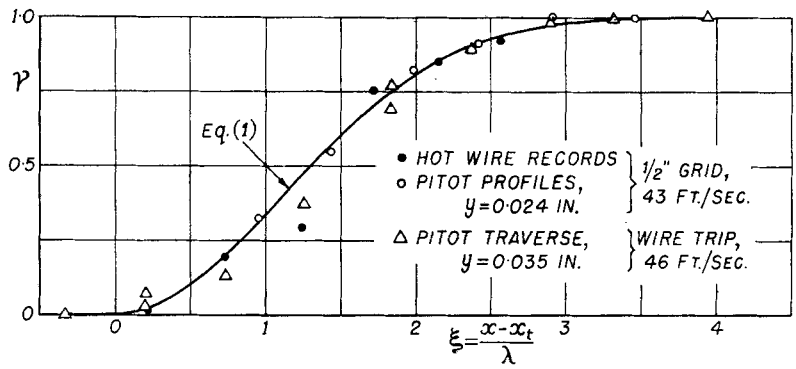

Figure 16. Estimation of γ using a Pitot tube.

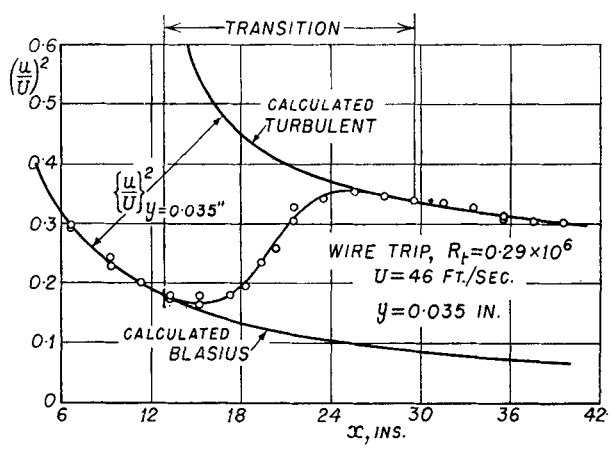

Figure 17. Pitot traverse along plate to estimate γ.

laminar. Incidentally, a simple method of obtaining the 'turbulent' curve in figure 17 is to plot the measured fully-turbulent points on logarithmic paper against $(x-x_t)$ and draw a straight line through them extending upstream. This line then gives the $(u/U)_T$ values for the γ determination in the transition region. This procedure gives good results and would be completely justified if the turbulent profiles followed a power law with a constant index throughout. The values of the intermittency obtained from this experiment are also plotted in figure 16.

Concluding remarks

In spite of the origin of turbulence remaining obscure, Emmons' picture of transition in a laminar boundary layer supplemented by experimental information allows a detailed physical model of the process to be set up. From this a relatively adequate calculation of the macroscopic effects can be carried out.

One of us (R. N.) wishes to acknowledge his indebtedness to the National Institute of Sciences of India for a Fellowship held during the course of this research.

References

Burgers, J. M. 1925 *Proc. 1st Internat. Cong. Appl. Mech., Delft,* 113.

Chapman, D. R. & Kester, R. H. 1933 *J. Aero. Sci.* **20,** 441.

Charters, A. C. 1943 *Nat. Adv. Comm. Aero., Wash., Tech. Note* no. 891.

Clauser, F. H. 1956 Article in *Advances in Applied Mechanics,* Vol. 4. New York : Academic Press.

Coles, D. 1954 *J. Aero. Sci.* **21,** 433.

Corrsin, S. & Kistler, A. L. 1954 *Nat. Adv. Comm. Aero., Wash., Tech. Note* no. 3133.

Dhawan, S. 1953 *Nat. Adv. Comm. Aero., Wash., Rep.* no. 1121.

Dryden, H. L. 1953 *J. Aero. Sci.* **20,** 477.

Emmons, H. W. 1951 *J. Aero. Sci.* **18.** 490.

Frankl, F. & Voishel, V. 1943 *Nat. Adv. Comm. Aero., Wash., Tech. Mem.* no 1053.

Gazley, C., Jr. 1953 *J. Aero. Sci.* **20,** 19.

Goldstein, S. (Ed.) 1938 *Modern Developments in Fluid Dynamics,* Vol. 2. Oxford University Press.

Hama, F. R., Long, J. D. & Hagerty, J. C. 1957 *J. Appl. Phys.* **28,** 388.

Higgins, R. W. & Pappas, C. C. 1951 *Nat. Adv. Comm. Aero., Wash., Tech. Note* no. 2351.

Hunsaker, J. C. 1939 *J. Aero. Sci.* **6,** 104.

Lees, L. 1952 *Consolidated Aircraft Corporation Rep.* no ZA–7–006.

Liepmann, H. W. 1945 *Nat. Adv. Comm. Aero., Wash., A.C.R.* no. 4J28.

Lin, C. C. 1955 *The Theory of Hydrodynamic Stability.* Cambridge University Press.

Mitchner, M. 1954 *J. Aero. Sci.* **21,** 350.

Narasimha, R. 1957 *J. Aero. Sci.* **24,** 711.

Persh, J. 1955 *J. Aero. Sci.* **22,** 443.

Schubauer, G. B. & Klebanoff, P. S. 1955 *Nat. Adv. Comm. Aero., Wash., Tech. Note* no. 3489.

Schubauer, G. B. & Skramstad, H. K. 1947 *J. Aero. Sci.* **14,** 69.

Schlichting, H. 1955 *Boundary Layer Theory.* London : Pergamon Press.

Shoulberg, R. H., Hill, J. A. R. & Rivas, M. A., Jr. 1954 *J. Aero. Sci.* **21,** 763.

Silverstein, A. & Becker, J. V. 1939 *Nat. Adv. Comm. Aero., Wash., Rep.* no. 637.

Tani, I. & Hama, F. R. 1953 *J. Aero. Sci.* **20,** 289.

Winter, K. G., Scott-Wilson, J. B. & Davies, F. V. 1954 *Aero. Res. Counc., Lond., Curr. Pap.* no. 212.

Wright, E. A. & Bailey, G. W. 1939 *J. Aero. Sci.* **6,** 485.